Available online at www.sciencedirect.com
SCIENCE DIRECT®
Journal of Magnetic Resonance 160 (2003) 161–165
JMR Journal of Magnetic Resonance
www.elsevier.com/locate/jmr

End-to-end correlation for a C-12 hydrocarbon chain

Shawn Wagner,[a] Alexander A. Nevzorov,[b] Jack H. Freed,[b] and Robert G. Bryant[a,*]

[a] *Department of Chemistry, University of Virginia, Charlottesville, VA 22904-4319, USA*
[b] *Department of Chemistry, Cornell University, Ithaca, NY 14853, USA*

Received 27 September 2002

Abstract

The ^{19}F nuclear spin-lattice relaxation rate constants were measured as a function of magnetic field strength for 1,12-diaminododecane labeled at one end with a nitroxide radical and at the other with a trifluoromethyl group. The magnetic relaxation dispersion profile (MRD) reports the spectral density function appropriate to the end-to-end correlation function for the doubly labeled molecule. After extrapolation to zero concentration to eliminate the intermolecular relaxation contribution to relaxation, the resulting intramolecular MRD profile was compared with several model approaches. The rotational model for the spectral density functions as included in the Solomon–Bloembergen–Morgan equations does not describe the data well. The earlier model of Freed for nuclear spin relaxation induced by a freely diffusing paramagnetic co-solute is not rigorous for this case because the paramagnet is tethered to the observed nuclear spin and only a restricted space in the immediate vicinity of the nuclear spin is accessible for pseudo-translational diffusion of one end of the molecule with respect to the other. A generalization of the Torrey model for magnetic relaxation by translational diffusion developed by Nevzorov and Freed, which includes the effect of restrictions imposed by the finite length of the chain, describes the experiment within experimental errors. A simple modification of the Hwang–Freed model that does not specifically include the dynamical effects of the finite tether also provides a good approximation to the data when the tether chain is sufficiently long.

Keywords: Spin-lattice relaxation; Magnetic relaxation dispersion; Spectral density; Tethered diffusion

1. Introduction

Nuclear spin-lattice relaxation rate constants are proportional to the Fourier transform of the autocorrelation function characterizing the fluctuations that modulate magnetic interactions at the position of the observed nuclear spin, usually caused by rotational and translational diffusion [1]. The effects of local internal motion may become important in large molecules, and, depending on the degree of segmental freedom sensed at the site of an observed nuclear spin, the effective correlation time may or may not simply reflect the global rotational reorientation of the molecule [2–11]. In the case of large globular molecules such as proteins, side chain motion may provide a complex spectral density function that contains the consequences of both the high frequency local motions as well as the overall rotational reorientation of the macromolecule. In this case, the major effect of the high frequency motion is that at smaller values of the Larmor frequency, the spin-lattice relaxation rate is scaled by a factor directly related to a generalized order parameter [3]. Although more detailed analysis is possible [12–14], the details of the high frequency motion are not available from measurements based only on nuclear spins at generally accessible magnetic field strengths.

In the case where a nuclear spin is relaxed by dipolar coupling to an electron spin, the relaxation equation contains terms that involve both the nuclear and the electron Larmor frequency. Because the electron Larmor frequency is larger than the nuclear Larmor frequency by the ratio of the magnetogyric ratios, ($\gamma_e/\gamma_H = 658$), the nuclear spin relaxation may probe spectral density functions at frequencies in the range of hundreds of GHz or time scales of order 1 ps. Therefore,

* Corresponding author. Fax: 1-434-924-3567.
E-mail address: rgb4g@virginia.edu (R.G. Bryant).

1090-7807/03/$ - see front matter © 2003 Elsevier Science (USA). All rights reserved.
doi:10.1016/S1090-7807(02)00143-X

nuclear magnetic relaxation dispersion (MRD) measurements in paramagnetic molecules provide an excellent approach to studying both inter and intramolecular reorientation in small as well as large molecules [15–20].

In the present study, the strategy was to label the ends of an alkane chain with a unique nuclear spin and the other end of the molecule with a stable electron magnetic moment. The use of a nitroxide spin-label provides the molecule with a dipole–dipole coupling between the observed fluorine nucleus and the electron spin, which has a spin-lattice relaxation time that is long compared with the translational or rotational correlation times of the molecule. Because the electron spin relaxation times are long compared to intra and intermolecular correlation times, the MRD profiles provide a map of the spectral density functions that monitor the end-to-end correlation in the molecule. For the ^{12}C molecule, this reorientation may involve rotational motions of all or part of the molecule as well as fluctuations in the end-to-end separation of the two spin labels in the molecule.

Fluorescence spectroscopy may report end-to-end correlations based on quenching by energy transfer between chromophores situated at the ends of a molecule like the one studied here [21–27]. A fundamental difference is that the fluorescence lifetime may contribute and interfere with to the effective correlation sampling window in the range of tens of nanoseconds; however, the nuclear spin relaxation rate constants represent long time measurements that sample the effects of the molecular dynamics over the time of the relaxation period, which is the order of tens to hundreds of ms. These two approaches are, therefore, different but complementary.

2. Experimental

Trifluoroaminododecanamide-tempo was prepared by reacting 12-aminododecanoic acid (1.0 g 95% purity, Aldrich Chemical, Milwaukee, WI) with trifluoroacetic anhydride (0.98, Aldrich, g 99% purity) in 50 mL methylene chloride. The product crystallized as solvent was removed by rotary evaporation and the solution stored at 0 °C for 12 h after which water was added to crystallize additional product with a total yield of 83%. The product (0.2 g) was reacted with 0.11 g of 4-amino-tempo and a 5-fold excess of 1,3-diisopropylcarbodiimide in 10 mL methylene chloride. After stirring for 4 h, the solution was evaporated under vacuum to yield a red-orange oil. The product was dissolved in a 60:40 mixture of hexanes and acetone, and passed down a G-25 silica gel column. The first orange band was collected and lyophilized for 24 h to a red-orange oil in 28% yield. An aliquot of the sample was used to confirm two exchangeable amide peaks in the ^1H NMR spectrum.

^{19}F spin-lattice relaxation rates were measured using a spectrometer constructed in this laboratory and described previously. The spectrometer utilizes a 7 T magnet Magnex (Oxford, UK) separated by an iron shield from a GMW (San Carlos, CA) 4-in. electromagnet. Samples are polarized in the 7 T magnet, pneumatically moved to the satellite field where spins are permitted to relax for a variable time after which the sample is pneumatically moved back to the 7 T magnet where it is sampled using conventional high resolution NMR techniques. Because the equilibrium magnetization in the satellite field is significantly less than that in the polarization-detection field of 7 T, generally no initial rf pulse is employed prior to the sample movement. Typically 16 transients were averaged for each spectrum, and 28 relaxation recovery times were employed at each magnetic field strength to define the spin-lattice relaxation rate constant.

3. Results

The ^{19}F MRD profile for the doubly spin labeled C-12 diamide is shown in Fig. 1 for concentrations from 10 to 30 mM in acetone as the solvent. The signal-to-noise ratio does not increase significantly with increasing concentration because the intermolecular contribution to the relaxation rate increases which decreases the detectable signal because of the constant sample transit times. Relaxation during the sample transit from one magnet to the other is rapid in the low field regions of the sample transit, which is a limitation of sample shuttle relaxometry. The total observed relaxation rates

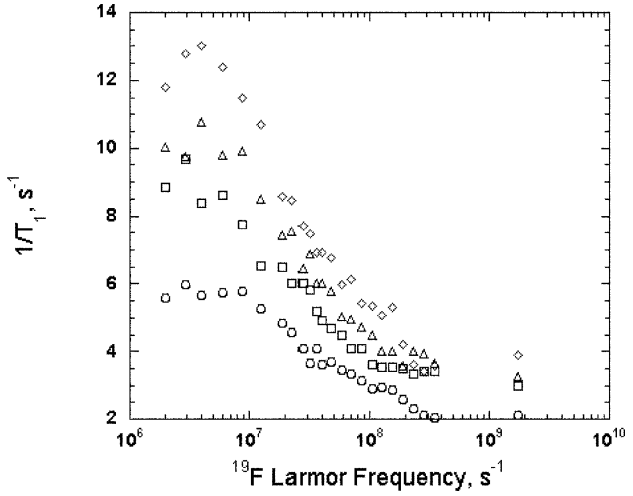

Fig. 1. ^{19}F nuclear spin-lattice relaxation rate constants for a terminal trifluoromethyl group in a C_{12} molecule labeled at the other terminus with a nitroxide radical as a function of the magnetic field strength represented as the fluorine radial Larmor frequency. Data were taken at ambient laboratory temperature in a shuttle instrument employing two magnets previously described [37]. The observed solute concentrations were: (○) 10 mM, (□) 20 mM, (△) 25 mM, (◇) 30 mM in acetone.

are a sum of inter- and intramolecular electron–nuclear dipolar contributions. The intramolecular contribution at each field strength was deduced by extrapolating the paramagnetic contribution to the relaxation rate to zero solute concentration. Because errors are significant in this experiment at the current level of technology, we utilized a 3-point smoothing process where individual relaxation rates in the dispersion profile were reconstructed using a 25% weight of the $n-1$ and $n+1$ points and 50% weight of the nth point. When tested against simulated data with simulated intra- and intermolecular correlation times of 20 and 40 ps, respectively, this procedure provided insignificant distortion of the MRD profile. The resulting MRD profile extrapolated to zero solute concentration is shown in Fig. 2.

The shape of the relaxation profile at infinite dilution is compared with three models shown in Fig. 2. The magnetic field dependence of the spin-lattice relaxation rate predicted by the standard Solomon–Bloembergen–Morgan (SBM) relaxation equations, which assume a rotational correlation of the dipolar coupling, is shown as the dashed line assuming an intermoment distance of 10.8 Å and an effective correlation time of 16 ps. In spite of the scatter in the extrapolated data points, the SBM model represents a poor approach to the data, which are expected because of the significant internal segmental motion between the chain ends.

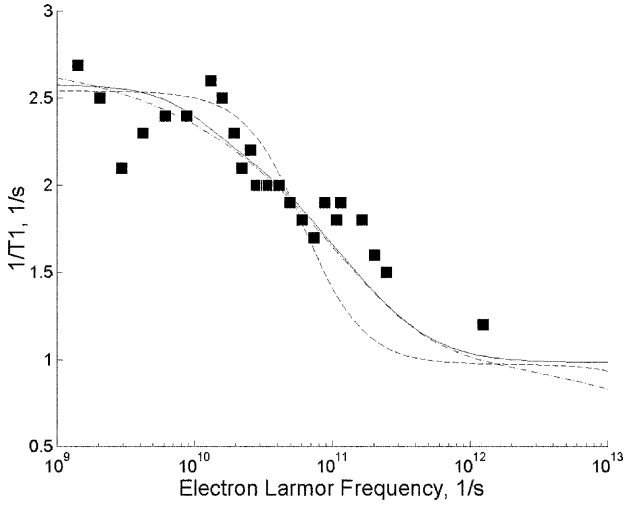

Fig. 2. The magnetic field dependence of the ^{19}F spin-lattice relaxation rate constant is shown as a function of magnetic field strength in the limit of infinite dilution. The solid curve was calculated using the Nevzorov–Freed model with a relative translational diffusion constant of $9.5 \times 10^{-9}\,m^2\,s^{-1}$ and a distance of closest approach of $3.08 \times 10^{-10}\,m$. The dashed line was computed using the Solomon, Bloembergen, Morgan equations for paramagnetic relaxation with a correlation time of 16 ps, and an intermoment separation of $10.77 \times 10^{-10}\,m$. The dash–dot line was computed using the Hwang–Freed model and the same parameters as in the Nevzorov–Freed calculation.

A better approach is to recognize that the time dependence of the radial vector connecting the two spins dominates the magnetic fluctuations at the fluorine site. The fluctuations in this radial vector will may be approximated by translational diffusion wherein this radial vector is constrained in its length by the length of the fully extended molecule so that the electron spin can never get infinitely far away from the nuclear spin. Although theoretical approaches by Hwang and Freed [28] and Ayant et al. [29] have provided closed form solutions to the intermolecular relaxation induced by the relative translation of spins coupled by the dipole–dipole interaction, the present situation is somewhat different because the space explored by the relative motion of the two coupled spins is constrained at both short and long distances. Recently, Nevzorov and Freed [6,7] have considered specifically the problem of spin–dipole–dipole coupling modulated by translational diffusion constrained by a tether. Related problems have been considered in the context of chemically induced dynamic polarization experiments [30–32]. This approach is based on expanding the density matrix in symmetry adapted basis set of eigenoperators following Banwell and Primas [33], and considering the coupled equations of motion for the coefficients of the eigenoperator expansion. This strategy permits one to follow multiple coherence pathways as well as relaxation. The stochastic Liouville equation is solved for constrained translational diffusion [6] using methods closely related to those of Hwang and Freed [28]. The solid line shown in Fig. 2 was computed using a numerical solution of this model with a distance of closest approach of $3.08 \times 10^{-10}\,m$ and a relative diffusion constant of $9.5 \times 10^{-9}\,m^2\,s^{-1}$.

Fig. 2 also shows a line computed using the theory of Hwang and Freed where the effect of the tether was approximated by using a relative spin concentration based on the spherical molecular volume described by taking as the radius the maximum value of the intermoment radial vector in the fully extended configuration. In order to better approximate the experimental results, we needed to divide this concentration by an arbitrary factor of 1.2. This factor corresponds to only a 6% increase in the effective radius of the volume explored by the ends of the molecule compared with that estimated from the molecular modeling program Spartan. This modified Hwang–Freed model differs from the Nevzorov–Freed model in that it neglects the dynamical effects of the outer bound or the tether. The near agreement for larger values of the maximum value of the intermoment radial vector shows that this dynamical effect becomes small for increasing tether lengths as expected. Although sufficient to show that a diffusion model is clearly superior to the SBM model, the data do not provide a rigorous test of, or distinction between, the details of the translational models.

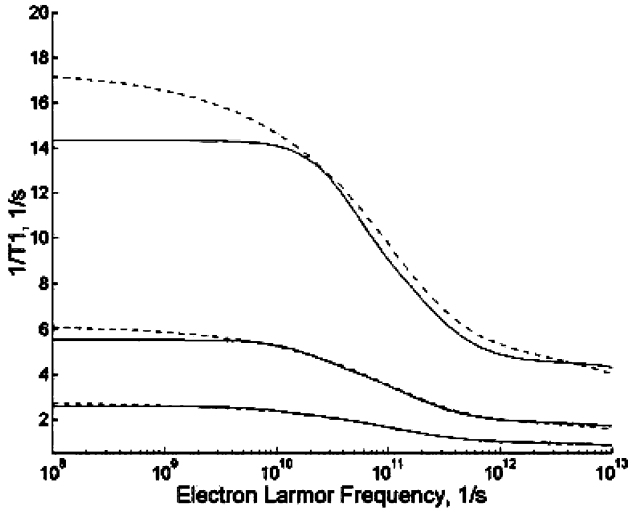

Fig. 3. Calculation of the paramagnetic contribution to nuclear spin-lattice relaxation rate constants using the Hwang–Freed (dash–dot), and Nevzorov–Freed (solid) models for three choices of the maximum end-to-end distance: 24.5 Å, (bottom), 18.2 Å (middle), and 12.8 Å (top).

Fig. 3 shows a comparison of the two translational theories for several choices of the maximum end-to-end length. In all cases, the same values of the translational diffusion constant and the distance of closest approach were used, and the volume explored by the spin-label, which defines the effective concentration of paramagnetic center in the Hwang-Freed model, was taken as 1/1.2 times the spherical volume with the radius given by the maximum separation of the observed fluorine and the nitroxide oxygen as determined by the all trans configuration of the hydrocarbon chain as noted above. The agreement in the range of the inflection is excellent and most data could not distinguish between the two models. The Hwang–Freed model yields a larger value of the low-field limiting relaxation rate constant as expected because the integration that leads to the spectral density includes contributions between the tether length and infinity. However, for the ratio of the maximum end-to-end length divided by the distance of closest approach greater than approximately 5, the analytical solution provided by the Hwang–Freed model provides a remarkably accurate characterization of the spin-lattice relaxation.

Two parameters determine the relaxation dispersion amplitude and inflection point, the distance of closest approach and the relative translational diffusion constant. The distance of closest approach is approximately what is expected based on the sum of van der Waals radii and is similar to values obtained in other studies [15,34]. The relative translational diffusion constant is largely determined by the inflection point of the relaxation dispersion, which yields an apparent translational diffusion constant of $7 \times 10^{-10}\,m^2\,s^{-1}$. This value appears to be larger than expected. The translational diffusion constants for acetic acid, benzoic acid, nitrobenzene and tetrachloromethane in acetone range from 2.62 to $3.77 \times 10^{-10}\,m^2\,s^{-1}$ [35]. The present experiments report the *relative* translational diffusion constant, which is the sum of the diffusion constants that characterize the motion of each dipole moment in the interacting pair. Thus, the relative translational diffusion constant derived from the present experiments should be approximately a factor of 2 larger than the self-diffusion constants for these simpler solutes, which it is. Of course, the parameter derived from the present experiment has the units of a translational diffusion constant, but does not characterize bulk transport in the medium. The possibility that local translational rearrangements may be more rapid than bulk transport measurements would imply has been noted based on simulations [36].

In summary, the relaxation dispersion measurements on an end-labeled hydrocarbon provide a test of relaxation theories for small molecules in liquids. The use of the paramagnetic contribution to the nuclear spin relaxation provides a direct probe of the correlation functions in the range from microseconds to picoseconds, and we find that for a freely jointed hydrocarbon chain in acetone, the Nevzorov–Freed models provide a good description of the relaxation profile. Comparison of this model for relative diffusion of spins on a tether with a simpler modified model that does not include the dynamical effects of the tether in detail shows that for lengths in excess of approximately five times the distance of closest approach of the spins, the Hwang–Freed model provides an excellent and simple description of the data.

Acknowledgments

This work was supported by the University of Virginia, and grants to RGB from the National Institutes of Health (GM54067) and grants to JHF from the National Institutes of Health NCRR, and the National Science Foundation.

References

[1] A. Abragam, in: The Principles of Nuclear Magnetism, Clarendon Press, Oxford, 1961, p. 386 (Chapter VIII).
[2] G. Lipari, A. Szabo, Model-free approach to the interpretation of nuclear magnetic resonance relaxation in macromolecules. 2. Analysis of experimental results, J. Am. Chem. Soc. 104 (1982) 4559–4570.
[3] G. Lipari, A. Szabo, Model-free approach to the interpretation of nuclear magnetic resonance relaxation in macromolecules. 1. Theory and range of validity, J. Am. Chem. Soc. 104 (1982) 4546–4559.
[4] D.E. Woessner, J. Chem. Phys. 37 (1962) 647–654.

[5] J.H. Freed, Stochastic-molecular theory of spin-relaxation for liquid crystals, J. Chem. Phys. 66 (9) (1977) 4183–4199.
[6] A.A. Nevzorov, J.H. Freed, Spin relaxation by dipolar coupling: from motional narrowing to the rigid limit, J. Chem. Phys. 112 (2000) 1413–1424.
[7] A.A. Nevzorov, J.H. Freed, Dipolar relaxation in a many-body system of spins 1/2, J. Chem. Phys. 112 (2000) 1425–1443.
[8] V. Tugarinov, Y.E. Shapiro, Z. Liang, J.H. Freed, E. Meirovitch, A novel view of domain flexibility in *E. coli* adenylate kinase based on structural mode-coupling (15)N NMR relaxation, J. Mol. Biol. 315 (2) (2002) 155–170.
[9] Y.E. Shapiro, E. Kahana, V. Tugarinov, Z. Liang, J.H. Freed, E. Meirovitch, Domain flexibility in ligand-free and inhibitor-bound *Escherichia coli* adenylate kinase based on a mode-coupling analysis of ^{15}N spin relaxation, Biochemistry 41 (20) (2002) 6271–6281.
[10] V. Tugarinov, Y.E. Shapiro, Z. Liang, J.H. Freed, E. Meirovitch, A novel view of domain flexibility in *E. coli* adenylate kinase based on structural mode-coupling ^{15}N NMR relaxation, J. Mol. Biol. 315 (2) (2002) 155–170.
[11] V. Tugarinov, Z. Liang, Y.E. Shapiro, J.H. Freed, E. Meirovitch, A structural mode-coupling approach to 15N NMR relaxation in proteins, J. Am. Chem. Soc. 123 (13) (2001) 3055–3063.
[12] Y.E. Shapiro, E. Kahana, V. Tugarinov, Z. Liang, J.H. Freed, E. Meirovitch, Domain flexibility in ligand-free and inhibitor-bound *Escherichia coli* adenylate kinase based on a mode-coupling analysis of 15N spin relaxation, Biochemistry 41 (20) (2002) 6271–6281.
[13] V. Tugarinov, Z. Liang, Y.E. Shapiro, J.H. Freed, E. Meirovitch, A structural mode-coupling approach to 15N NMR relaxation in proteins, J. Am. Chem. Soc. 123 (13) (2001) 3055–3063.
[14] V. Tugarinov, Y.E. Shapiro, Z. Liang, J.H. Freed, E. Meirovitch, A novel view of domain flexibility in *E. coli* adenylate kinase based on structural mode-coupling ^{15}N NMR relaxation, J. Mol. Biol. 315 (2) (2002) 155–170.
[15] T.R.J. Dinesen, S. J., M. L., S. Wagner, R.G. Bryant, ^{19}F and ^{1}H magnetic relaxation dispersion determination of the translational encounter between ionic salts and nitroxide free radicals in aqueous solution, J. Phys. Chem. A 103 (1999) 782–786.
[16] J.-P. Korb, R.G. Bryant, The physical basis for the magnetic field dependence of spin-lattice relaxation rates in proteins and tissues, J. Chem. Phys. 115 (2001) 10964–10974.
[17] S. Stapf, R. Kimmich, Molecular dynamics in confined monomolecular layers. A field-cycling nuclear magnetic resonance relaxometry study of liquids in porous glass, J. Chem. Phys. 103 (6) (1995) 2247–2250.
[18] R. Kimmich, R.O. Seitter, U. Beginn, M. Moller, N. Fatkullin, Field-cycling NMR relaxometry of polymers confined to artificial tubes: verification of the exponent 3/4 in the spin-lattice relaxation dispersion predicted by the reptation model, Chem. Phys. Lett. 307 (3–4) (1999) 147–152.
[19] R. Kimmich, K. Gille, N. Fatkullin, R. Seitter, S. Hafner, M. Muller, Field-cycling nuclear magnetic resonance relaxometry of thermoreversible polybutadiene networks, J. Chem. Phys. 107 (15) (1997) 5973–5978.
[20] R. Kimmich, N. Fatkullin, R.O. Seitter, K. Gille, Chain dynamics in entangled polymers: power laws of the proton and deuteron spin-lattice relaxation dispersions, J. Chem. Phys. 108 (5) (1998) 2173–2177.
[21] E. Haas, M. Wilcheck, E. Katchalski-Katzir, I.A. Steinberg, Distribution of end-to-end distances of oligopeptides in solution as estimated by energy transfer, Proc. Natl. Acad. Sci. 72 (1975) 1807–1811.
[22] A. Grinvald, E. Haas, I.Z. Steinberg, Evaluation of the distribution of distances between energy donors ad acceptors by fluorescence decay, Proc. Natl. Acad. Sci. 69 (1972) 2273–2277.
[23] E. Haas, E. Katchalski-Katzir, I.Z. Steinberg, Brownian motion of the ends of oligopeptide chains in solution as estimated by energy transfer between chain ends, Biopolymers 17 (1978) 11–31.
[24] J.R. Lakowicz, W. Wiczk, I. Gryczynski, H. Szmacinski, M.L. Johnson, Influence of end-to-end diffusion on intramolecular energy transfer as observed by frequency-domain fluorometry, Biophys. Chem. 38 (1–2) (1990) 99–109.
[25] I. Gryczynski, W. Wiczk, M.L. Johnson, H.C. Cheung, C.K. Wang, J.R. Lakowicz, Resolution of end-to-end distance distributions of flexible molecules using quenching-induced variations of the Forster distance for fluorescence energy transfer, Biophys. J. 54 (4) (1988) 577–586.
[26] J.R. Lakowicz, J. KuSba, H. Szmacinski, I. Gryczynski, P.S. Eis, W. Wiczk, M.L. Johnson, Resolution of end-to-end diffusion coefficients and distance distributions of flexible molecules using fluorescent donor–acceptor and donor–quencher pairs, Biopolymers 31 (12) (1991) 1363–1378.
[27] B.P. Maliwal, J. KuSba, W. Wiczk, M.L. Johnson, J.R. Lakowicz, End-to-end diffusion coefficients and distance distributions from fluorescence energy transfer measurements: enhanced resolution by using multiple acceptors with different Förster distances, Biophys. Chem. 46 (3) (1993) 273–281.
[28] L.-P. Hwang, J.H. Freed, Dynamic effects of pair correlation functions on spin relaxation by diffusion in liquids, J. Chem. Phys. 63 (1975) 4017–4025.
[29] Y. Ayant, E. Belorizky, J. Alizon, J. Gallice, Calculation of spectral density resulting from random translational movement with relaxation by magnetic dipolar interaction in liquids, J. Phys. I 36 (10) (1975) 991–1004.
[30] M.D.E. Forbes, S.R. Ruberu, Time-resolved EPR spectra of short biradicals (1,3-1,8-) in solution. The interconnecting roles of the external magnetic field, dipolar coupling, exchange interaction and molecular motion in the spin polarization and relaxation mechanisms, J. Phys. Chem. 97 (1993) 13223–13233.
[31] F.J.J. de Kanter, J.A. den Hollander, A.H. Huizer, R. Kaptein, Biradical CIDNP and the dynamics of polymethylene chains, Mol. Phys. 34 (1777) 857–874.
[32] S. Stob, J. Kemmink, R. Kaptein, Intramolecular electron transfer in flavin adenine dinucleotide. Photochemically induced dynamic nuclear polarization study at high and low magnetic fields, J. Am. Chem. Soc. 111 (18) (1989) 7036–7042.
[33] C.N. Banwell, H. Primas, On the analysis of high-resolution nuclear magnetic resonance (N.M.R.) spectra. I. Methods of calculating N.M.R. spectra, Mol. Phys. 6 (1963) 225–256.
[34] C.F. Polnaszek, R.G. Bryant, Nitroxide radical induced solvent proton relaxation: measurement of localized translational diffusion, J. Chem. Phys. 81 (1984) 4038–4045.
[35] D.R. Lide, in: D.R. Lide (Ed.), CRC Handbook of Chemistry and Physics, seventy-sixth ed., CRC Press, New York, 1995, pp. 6–257.
[36] J.A. Nairn, C.L. Braun, Monte Carlo simulations of the rate of intramolecular end-to-end contact in alkane chains, J. Chem. Phys. 74 (1981) 2442–2449.
[37] S. Wagner, T.J.R. Dinesen, T. Rayner, R.G. Bryant, Magnetic relaxation dispersion measurements using a dual magnet system, J. Magn. Reson. 140 (1999) 172–178.